SJG
Scottish Journal of Geology

Research article

Published online January 10, 2018; updated January 30, 2018 https://doi.org/10.1144/sjg2017-010 | Vol. 54 | 2018 | pp. 37–49

Multi-stage pyrite genesis and epigenetic selenium enrichment of Greenburn coals (East Ayrshire)

Liam A. Bullock[1]*, John Parnell[1], Magali Perez[2], Adrian Boyce[3], Joerg Feldmann[2] & Joseph G.T. Armstrong[1]

[1] Department of Geology & Petroleum Geology, Meston Building, University of Aberdeen, King's College, Aberdeen AB24 3UE, UK
[2] Trace Element Speciation Laboratory (TESLA), Department of Chemistry, Meston Building, University of Aberdeen, King's College, Aberdeen AB24 3UE, UK
[3] Scottish Universities Environmental Research Centre, East Kilbride, Glasgow G75 0QF, UK
L.A.B., 0000-0001-9524-7206; A.B., 0000-0002-9680-0787; J.F., 0000-0002-0524-8254; J.G.T.A., 0000-0002-1342-3710
*Correspondence: liam.bullock@abdn.ac.uk

Abstract: Carboniferous coals of the Ayrshire Coalfield are enriched in selenium (Se) relative to average UK and world compositions, substituting for sulphur in pyrite. Greenburn surface mine coals are characterized by syngenetic concretionary pyrite (*c.* 15% total area), occurring as bedding-parallel banding, and later-formed (epigenetic) cross-cutting pyrite in cleats (*c.* 9% total area). In these, sulphur isotope compositions for both syngenetic and epigenetic pyrite include isotopically light and heavy variants, suggesting diagenetic and hydrothermal fluid formation. Late/post-Visean cleat-filling pyrite is enriched in Se (up to 266 ppm) compared to the earlier-formed material (Se up to 181 ppm).

Anomalous Se may have been sourced from near-by sulphidic Dalradian metamorphic rocks. Initial Se sequestration is associated with syngenetic pyrite mineralization, absorbed from seawater and pore waters, with additional Se introduced from fluids mobilized during epigenetic pyrite formation. Cleats from local brittle fracturing provided channels for fluid flow and a locus for precipitation of comparatively high-Se pyrite. Permian dolerite intrusions may have provided an enrichment source and/or fluid distribution mechanism. The Se concentrations of the Greenburn coals relate to multi-stage mineralization, with cleat-filling pyrite showing the highest Se content, and highlight the potential for high Se in similarly altered and fractured coal deposits worldwide.

Supplementary material: LA-ICP-MS maps for Fe, Se, Ag, As, Cu, Hg, Pb and Te for Greenburn coal samples from seams 9300 Lime and 6900 Burnfoot Bridge are available at https://doi.org/10.6084/m9.figshare.c.3967860

Received 29 July 2017; **revised** 17 October 2017; **accepted** 27 October 2017

The Ayrshire Coalfield, of Carboniferous age, is exposed across the county in SW Scotland and in surface coal mines, such as the Greenburn Mine Complex (operated by Kier Group; Figs 1–2), and hosts coals with a range of sulphur (S) and pyrite contents across a number of seams. Opencast coal sites in East Ayrshire allow for exceptional exposure and sampling of seams and strata (BGS online 2017). Seams that contain high pyrite content host strategic trace elements such as selenium (Se), important for developing low-carbon technologies such as photovoltaic solar cells (Talens Peiró *et al.* 2011; Ayres & Talens Peiró 2013; STDA 2013; Woodhouse *et al.* 2013; Lusty & Gunn 2014). Due to increasing demand and improved recovery worldwide, coal deposits have been identified as a potential resource for Se (UKERC 2012). Worldwide, coals generally contain 1.6–3 ppm Se (Bragg *et al.* 1998; Yudovich & Ketris 2006), although pyritic coals may host notably higher concentrations. In coals here, Se values in excess of the UK and Irish averages (3.9 ppm calculated from measurements by Bragg *et al.* (1998) and Spears (2015)) are considered high, and concentrations only slightly higher than this have important environmental implications (e.g. 4.2 ppm average Se in Chinese coals; Su *et al.* 1990; Bragg *et al.* 1998; Zheng *et al.* 1999; Zhu *et al.* 2012) relating to their mobility and release by natural weathering. Coal combustion has been damaging in coal mining regions, such as British Columbia, Canada (McDonald & Strosher 1998; Lemly 2004; Hendry *et al.* 2015), through the release of Se into the environment. Because Se can substitute for S and thus concentrate in pyrite, an understanding of the origins of pyrite in coals is important for the light it sheds on processes of Se enrichment. The pyritic coals of the Greenburn surface mine show evidence of multiple stages of pyrite formation, including banded syngenetic and cleat-filling pyrite hosted in systematic fractures in coal (Dron 1925; Laubach *et al.* 1998; Rippon *et al.* 2006). The aims of this study are: (1) to identify the origin of the pyrite in Greenburn coals; (2) to examine how the Se content relates to pyrite genesis, i.e. the relationship between syngenetic/epigenetic pyrite paragenesis and high Se concentrations; (3) to identify the potential sources and processes of Se enrichment in the Greenburn coals; and (4) to recognize any potential economic or environmental implications.

In addition to Se, a suite of other trace elements chemically related to Se, and elements associated with pyrite mineralization (e.g. As, Cd, Co, Fe, Hg, Mo, S, Ta, Te and Tl) were measured in whole-rock pyritic coal samples from the Greenburn mine. Variations in the S isotopic composition of

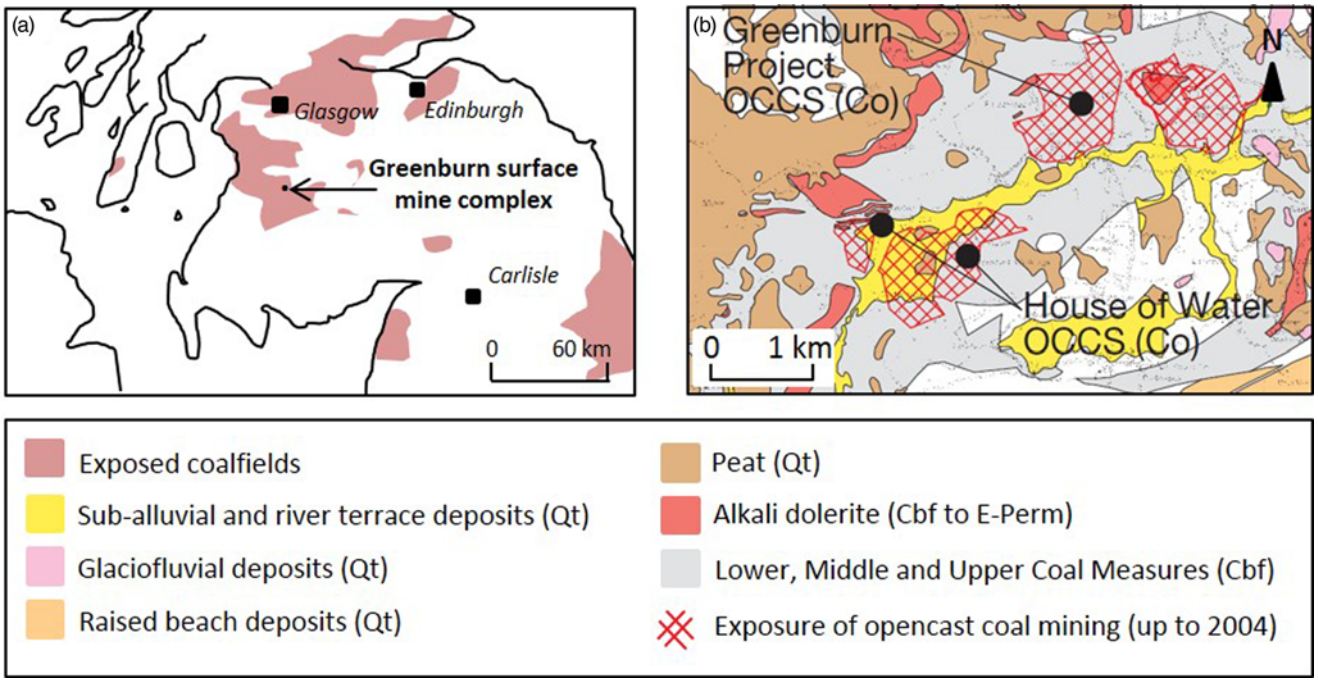

Fig. 1. (**a**) Southern Scotland and northern England coalfield exposure and locality of the Greenburn surface mine and (**b**) regional mineral resource geology of the Greenburn surface mine area (Smith *et al.* 2008). Qt, Quaternary deposits; Cbf, Carboniferous deposits; E-Perm, Early Permian deposits. House of Water opencast coal surface (OCCS) mine also shown on map.

pyrite were measured in order to provide insights into their origin. Light and variable S isotope compositions in pyrite have been used to infer the influence of sulphate-reducing bacteria (and subsequent Se precipitation by sulphate-reducing microbes in sampled coals), whereas heavier S isotope compositions indicate a non-biological origin (i.e. physical and chemical diagenesis). Laser ablation elemental mapping and line transect techniques have been applied to highlight significant Se concentrations, including zonation and higher content in syngenetic or epigenetic pyrite formation. Correlations between Se concentrations in different stages of formation provide insights into the mechanisms of preferential trace element accumulations in coal, important for assessment of the resource potential, environmental impact and detection of similar trace element-rich pyritic coal deposits.

Regional geology

The Ayrshire Coalfield forms part of the Coal Measures Supergroup, Carboniferous in age, which extends from the Midland Valley of Scotland, across the north of England to the English Midlands, South Wales and Kent. Ayrshire coals are generally classified as Lower, Middle and Upper Scottish Coal Measures (upper Westphalian A at the base, Westphalian B to Lower C; Figs 1–2) to the base of the Limestone Coal Formation (Pendleian, part of the Clackmannan Group) (Fielding 1982; Waters *et al.* 2007; Spears 2015). These rocks formed in a range of fluvial coastal plains, swamps, estuaries and deltas, with local environments including alluvial and lacustrine deposits, wetland forests and soils. Coals were typically formed in marginal coastal plains with lakes, swamps and deltas periodically inundated by the sea. Coal seams at the Greenburn mine comprise Lower and Middle Coal Measures, with some Upper Coal Measures, and form a broad synclinal basin, locally affected by fold and thrust faults with variable styles of displacement, as well as numerous Permian alkali dolerite sills (Fig. 1) (Tyrrell 1928; Walker & Patterson 1959; Smith *et al.* 2008). The Ayrshire Coalfield has a long history of deep and opencast coal mining, and was regarded as an important asset in South Ayrshire in the early twentieth century (Richey *et al.* 1925; Lebon 1933). Deep mining ceased in the 1980s, with opencast extraction continuing into the twenty-first century (Smith *et al.* 2008).

Methods

Coal samples ($n = 8$) span Westphalian A (Lower Coal Measures), B (Middle Coal Measures) and C (Upper Coal Measures), taken from exposures at Braehead Farm and Dalgig (Fig. 2). Sampled seams include, in stratigraphically descending order, 9600 Burnfoot Bridge, 9400 Little Cannel, 9450 Little Cannel Upper, 9300 Lime, 1940 Little Cannel Stringer, 1930 Lime Lower, 8700 Five Foot Lower, 8650 Eight Foot Upper, 8600 Eight Foot Lower and 6900 Knockshinnock (K.) Main Rider. (Fig. 2). The Se and associated trace element contents of samples of coal seams spanning the Upper, Middle and Lower Coal Measures ($n = 5$) were determined as part of a suite of 51 elements using inductively coupled plasma mass spectrometry (ICP-MS) at ALS Minerals (Loughrea, Ireland). Samples were milled and homogenized, and 0.25 g digested with aqua regia in a graphite heating block. The residue was diluted with deionized water, mixed and analysed using a Varian 725 instrument (Method code: ME-MS41). Results were corrected for spectral inter-element interferences. Measurement of four standards fell within pre-defined targets, and duplicate analyses for blanks, standards and repeat samples

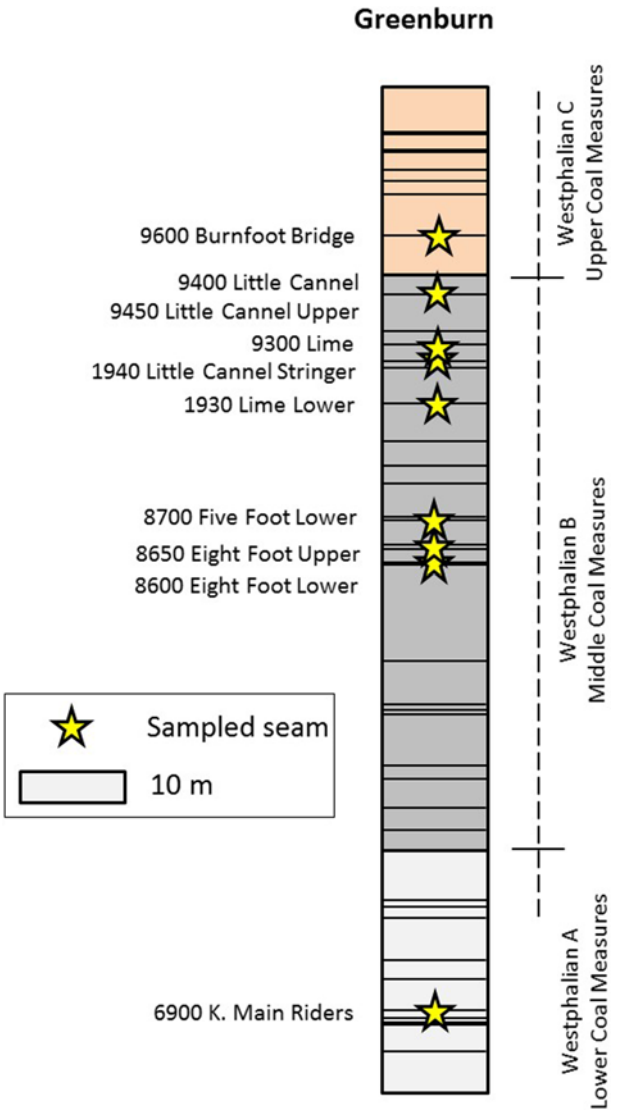

Fig. 2. Generalized stratigraphical section and sampled coal seams across three localities of the Greenburn surface mine (after Kier Mining 2009).

were all within 1% of each other. Sulphur and total organic carbon (TOC) content of select coal seams ($n = 7$) was measured using a LECO CS225 elemental analyser to a precision of ±0.05% based on two runs per sample. Analyses were run concurrently with C and S standards 501-024 (Leco Instruments, 3.23 ± 0.03% C, 0.047 ± 0.003% S, instrument uncertainty ± 0.05% C, ±0.002% S) and BCS-CRM 362 (Bureau of Analysed Samples Ltd, 1.48% S). The repeatability (based on three repeats of standards and blanks) of samples was consistently within 1%.

Pyrite samples ($n = 21$) from selected Greenburn coal seams ($n = 8$) were prepared for conventional S isotopic analysis by hand picking. Pyrite samples were combusted with excess Cu_2O at 1075°C in order to liberate the SO_2 gas under vacuum conditions. Liberated SO_2 gases were analysed on a VG Isotech SIRA II mass spectrometer, with standard corrections applied to raw $\delta^{66}SO_2$ values to produce True $\delta^{34}S$. Sulphur has five naturally occurring isotopes, four of which are stable (^{32}S [95% terrestrial abundance], ^{33}S, ^{34}S and ^{36}S) whereas ^{35}S is radiogenic. Stable isotope geochemistry is concerned primarily with the relative partitioning of isotopes among substances (i.e. changes in the ratios of isotopes), rather than their absolute abundances. The principal ratio of concern in sulphides is $^{34}S/^{32}S$, i.e. in the $\delta^{34}S$ notation, with parts per thousand or per mille (‰) variations from the V-CDT standard (Bottrell *et al.* 1994; Seal 2006). The standards employed were internationally certified reference materials NBS-123 and IAEA-S-3 (supplied by the IAEA) and Scottish Universities Environment Research Centre (SUERC) laboratory standard CP-1. These gave $\delta^{34}S$ values of +17.1‰, −31.2‰ and −4.6‰, respectively, with 1σ reproducibility, based on repeat analyses of the standards, better than ±0.2‰.

For laser ablation (LA-ICP-MS) mapping, transecting and quantification of pyrite in coal ($n = 2$), trace element analysis was performed using a New Wave Research laser ablation system UP 213 nm coupled to an ICP-MS Agilent 7900. Sample mapping was performed at a 10 Hz repetition rate, a spot size of 100 µm and an ablation speed of 50 µm s^{-1}. Each ablation was preceded by 15 s warm up, with a delay of 15 s applied between each ablation. The following isotopes were monitored (dwell time): ^{57}Fe (0.001 s), ^{65}Cu (0.001 s) ^{75}As (0.05 s), ^{78}Se (0.1 s), ^{82}Se (0.1 s), ^{107}Ag (0.1 s), ^{125}Te (0.1 s), ^{126}Te (0.1 s), ^{197}Au (0.1 s), ^{202}Hg (0.1 s), ^{208}Pb (0.05 s) and ^{209}Bi (0.1 s). NIST Glass 612 (NIST Gaithersburg MD) was used to optimize the ICP-MS parameters in order to reach the maximum sensitivity and to guarantee a low oxide formation. For that, the ratio $^{232}Th^{16}O+/^{232}Th+$ (as 248/232) was monitored and maintained below 0.3%. Hydrogen (3.5 ml min^{-1}) was used in the reaction cell to ensure that no interference could affect the Se measurement. Quantification was performed using the reference material MASS-1 Synthetic Polymetal Sulfide (USGS, Reston, VA). The ratio concentration (µg g^{-1})/counts per second was calculated from the standard MASS-1 and multiplied by the sample counts.

Results

Sample description and geochemistry

Greenburn coals are predominantly bituminous, and samples from seams 6900 K. Main Rider, 9300 Lime and 8700 Five Foot Lower contain abundant pyrite of two varieties: (1) disseminated and concretionary banded (bedding-parallel) pyrite and (2) discordant, typically vertical, cross-cutting pyrite (i.e. cleat-filling pyrite concentrated within small fractures; Fig. 3). The total proportional area of bedding-parallel pyrite in 9300 Lime and 6900 K. Main Rider pyritic coal samples is *c.* 13–15% (calculated from digitized images in Fig. 3 using *ImageJ* software), comprising *c.* 60–65% of total pyrite area. Cleat-filling pyrite comprises *c.* 6–9% of the total sample area and *c.* 30–35% of the total pyrite area.

The coals analysed exhibit a whole-rock range in Se content of 4.1–15.8 ppm ($n = 5$), with an average Se content of 9 ppm (Table 1). All samples show higher Se than UK and world averages (1.8 and 1.3 ppm, respectively; Spears & Zheng 1999; Ketris & Yudovich 2009; Yudovich & Ketris 2015). The higher pyrite content of samples is reflected in a higher S content (Table 2), with an average of 17.5% across samples ($n = 7$; average S content for seams also shown). Lower S coals show higher TOC (average 35.5%, maximum 71.8%), while more pyritic samples such as 8700 have the highest S content (33.9%). The more pyritic coals also show higher Se concentrations (seam 6900 = 15.4 ppm and seam

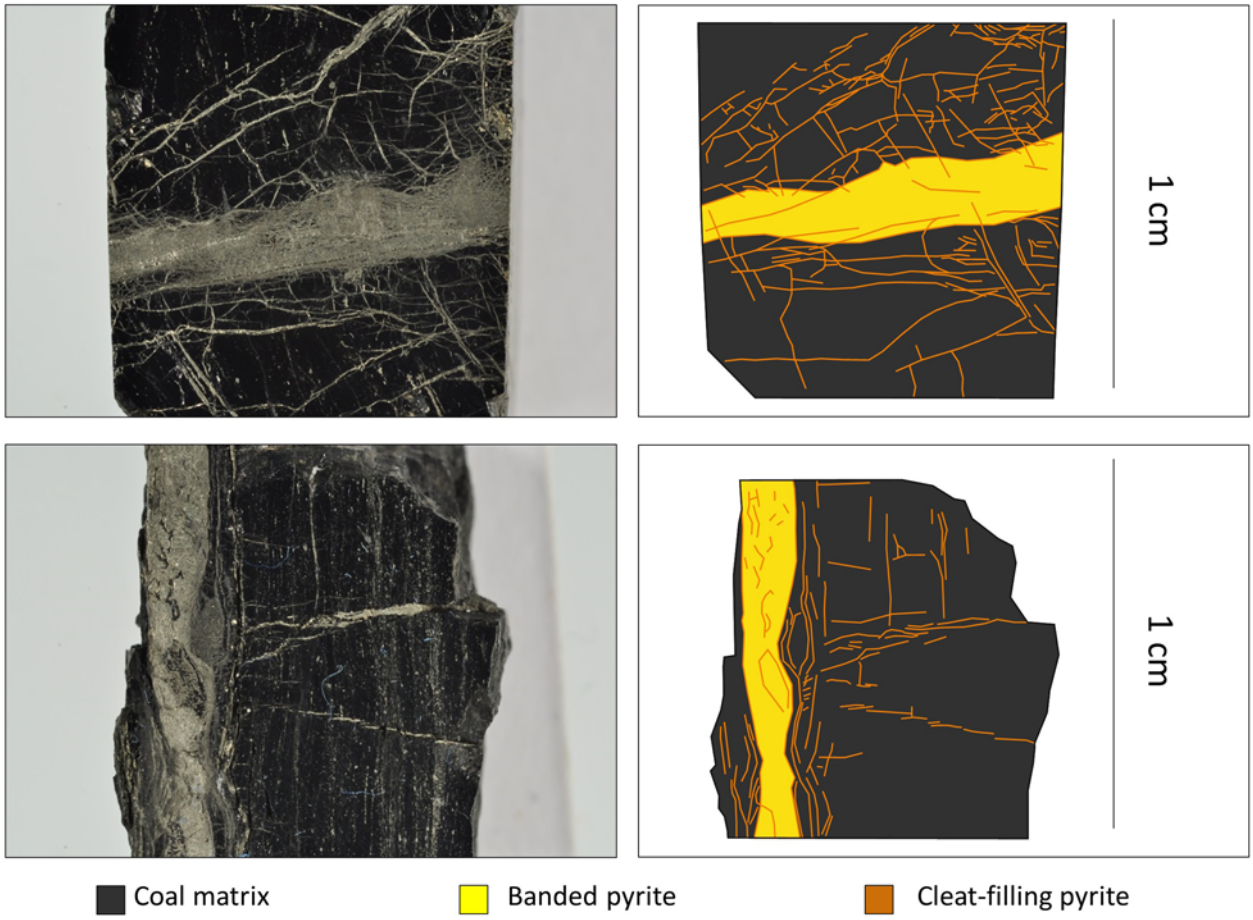

Fig. 3. Photographs and schematics of banded (yellow) and cleat-filling (orange) pyrite in Greenburn coals.

8700 = 15.8 ppm), together with elevated As (seam 6900 = 860 ppm and seam 8700 = 1700 ppm). The maximum Te value is 0.07 ppm, with other samples showing less than 0.02 ppm. Anomalous Pb (up to 1430 ppm) is evident in the Greenburn 9300 Lime coal seam. There are positive Se whole-rock correlations with As, Cd, Co, Hg, Ta and Tl (R^2 correlation values >0.8 for 5 samples, calculated by Microsoft Excel), typically associated with pyrite formation. Oxyanionic elements such as Se and As are common in pyrite, with heavy metals such as Co and Tl (Swaine 1990; Finkelman *et al.* 1999; Large *et al.* 2014). Trace elements, such as As, Hg, Co and Cd, are incorporated into the precursor iron monosulphide at an early stage (Large *et al.* 2014). As and Se readily substitute for S in pyrite, while Hg occurs as micro-inclusions, and may be introduced through hydrothermal fluids, or scavenged from gases by pyrite (Yudovich & Ketris 2006). Though Ta is more commonly associated with elements such titanium, or zirconium or with phosphates in coals, it may also substitute for Fe.

Trace element LA-ICP-MS mapping

Laser ablation ICP-MS maps (covering both banded and cleat-filling pyrite) show that trace elements concentrate in pyrite, with Se in greater abundance in cleat-filling pyrite (Figs 4–6). Trace element concentrations are generally low in the background coal matrix and high in the pyrite phases (see Supplementary material). Line transect profiles across pyrite types highlight the Se enrichment in cleat-filling pyrite (Fig. 5). The banded pyrite as a whole shows Se enrichment relative to the coal matrix, and cleats show higher intensity peaks. Fe is also high across cleats, and As replicates Se. Conversely, Te is low in both pyrite types, with lower peak intensities in pyrite compared to the coal matrix. With the exception of Bi and Te, cleat-filling pyrite generally contains higher trace element concentrations than banded pyrite that, in turn, contains higher trace elements than the background coal (Table 3). Quantification of LA-ICP-MS mapping reveals that cross-cutting cleats of the 9300 Lime coal contain a maximum Se content of up to 266 ppm, with typical concentrations of 157 ppm (Table 3; Fig. 6). Banded pyrite of the 9300 Lime coal commonly contains 60 ppm Se (maximum of 181 ppm), whereas the coal matrix contains only 15 ppm Se (Table 3), consistent with coal matrix whole rock concentrations. Of the two types of pyrite in the 6900 K. Main Rider coal, the banded pyrite contains 25 ppm Se (maximum 71 ppm), whereas cleat-filling pyrite contains up to 190 ppm Se (average 84 ppm Se; Table 3; Fig. 6). The coal matrix in these typically contains only 9 ppm Se (Table 3; Fig. 6). High Pb occurs in coal matrices associated with both syngenetic and epigenetic pyrite (see Supplementary material), typically concentrating in cleat-filling pyrite (averaging 638.5 ppm in 6900 Burnfoot Bridge cleat-filling pyrite).

Sulphur isotope compositions

The $\delta^{34}S$ values of Greenburn coal samples vary vertically, ranging from −26.3 to +18.4‰ (n = 21); Table 4 and Fig. 7).

Table 1. *Average whole-rock trace element concentrations of coals from sampled seams at Greenburn surface mine*

	Ag (ppm)	As (ppm)	Bi (ppm)	Cd (ppm)	Co (ppm)	Cu (ppm)	Fe (%)	Hg (ppm)	Mo (ppm)	Pb (ppm)	Se (ppm)	Ta (ppm)	Te (ppm)	Tl (ppm)
World Coal Clarke values	0.09	8.3	0.97	0.22	86	16	–	0.1	2.2	7.8	1.3	0.28	–	0.63
Ayrshire coals														
6900 K. Main Rider (pyrite-free)	1.19	82.9	0.01	0.05	45.3	15.4	2.2	0.5	5.0	39.1	5.0	0.02	0.01	0.3
6900 K. Main Rider (pyritic)	2.5	860.0	0.17	0.37	82.7	36.8	23.4	2.3	37.3	164	15.4	0.04	<0.01	2.4
9300 Lime	0.61	99.6	0.01	0.07	32.8	126.5	24.1	0.4	28.7	1430	4.7	0.02	<0.01	0.2
8700 Five Foot Lower	1.15	1700	0.04	0.68	131.5	59	26.4	1.6	99.6	209	15.8	0.05	0.02	1.8
8650 Eight Foot Upper	0.25	52.9	0.06	0.01	36.2	42.9	3.5	0.2	2.3	128	4.1	0.01	0.07	0.1

Coal Clarke values also shown (Ketris & Yudovich 2009; Yudovich & Ketris 2015).

Table 2. *S and TOC content (%) from selected Greenburn surface mine pyritic coal samples, and overall S content average (%) for sampled seams*

	Sample S (%)	Overall seam average S (%)	Sample TOC (%)
6900 K. Main Rider	20.6	1.0	43.7
1940 Little Cannel Stringer	8.4	6.7	50.5
8700 Five Foot Lower	33.9	4.0	15.9
8650 Eight Foot Upper	29.2	1.3	14.0
9300 Lime	28.7	3.7	13.9
9400 Little Cannel	1.7	4.0	71.8
9700 Lower Rigfoot	0.3	1.1	38.6

The overall average $\delta^{34}S$ composition is +2.7‰, with banded pyrite showing a slightly heavier average composition (+3.4‰; $n = 12$) compared to cleat-filling pyrite (+1.8‰; $n = 9$). Although samples are predominantly isotopically heavy (^{34}S-enriched), five of those analysed are isotopically light (^{32}S-enriched). These are concentrated within the Middle Coal Measures (Westphalian B), and occur in both banded and cleat-filling phases. Isotopic compositions become progressively heavier with depth across the Westphalian A and B coals. The lightest S isotope composition is from banded pyrite of the 1940 Little Cannel Stringer (Westphalian B), whereas the heaviest is from banded pyrite of the 6900 K. Main Rider seam (Westphalian A).

Discussion

Source of selenium

During the Carboniferous period, groundwaters drained through Dalradian metamorphic rocks. Dalradian rocks north of Ayrshire host pyritic and pyrrhotitic mineralization. Argyll Group sulphide mineralization at McPhun's Cairn shows Se content of up to 360 ppm in pyrite, and up to 790 ppm in chalcopyrite (Willan & Hall 1979; Willan 1980). The high Se content and susceptibility for mobility and fixation during the Carboniferous make the Dalradian rocks the most probable source of Se for Greenburn coals.

There are, however, several other potential sources in the Ayrshire region for the Se. These include deep and shallow igneous intrusions of the Midland Valley, including Ordovician volcanic rocks and selenide-bearing Devonian and Carboniferous sedimentary strata. Locally, East Ayrshire hosts a Devonian granodiorite (the Polshill Pluton), Late Silurian to Early Devonian granite and a Carboniferous to Permian gabbro. High-Se soils have been identified in the Midland Valley of western Scotland, the products of weathering of basaltic rocks and of Devonian Lower Old Red Sandstone (Shand *et al.* 2012). The Ordovician Marchburn Formation comprises basalt and microgabbro, and the Siluro-Devonian lavas of western Scotland (derived from enriched sub-continental mantle) contain up to 22.2 ppm Se (Thirlwall 1986). Basanitic and foiditic plugs and vents are also exposed in East Ayrshire, and localized sills from a volcanic plug may be responsible for the de-volatilization, destruction and fluid flow effects on

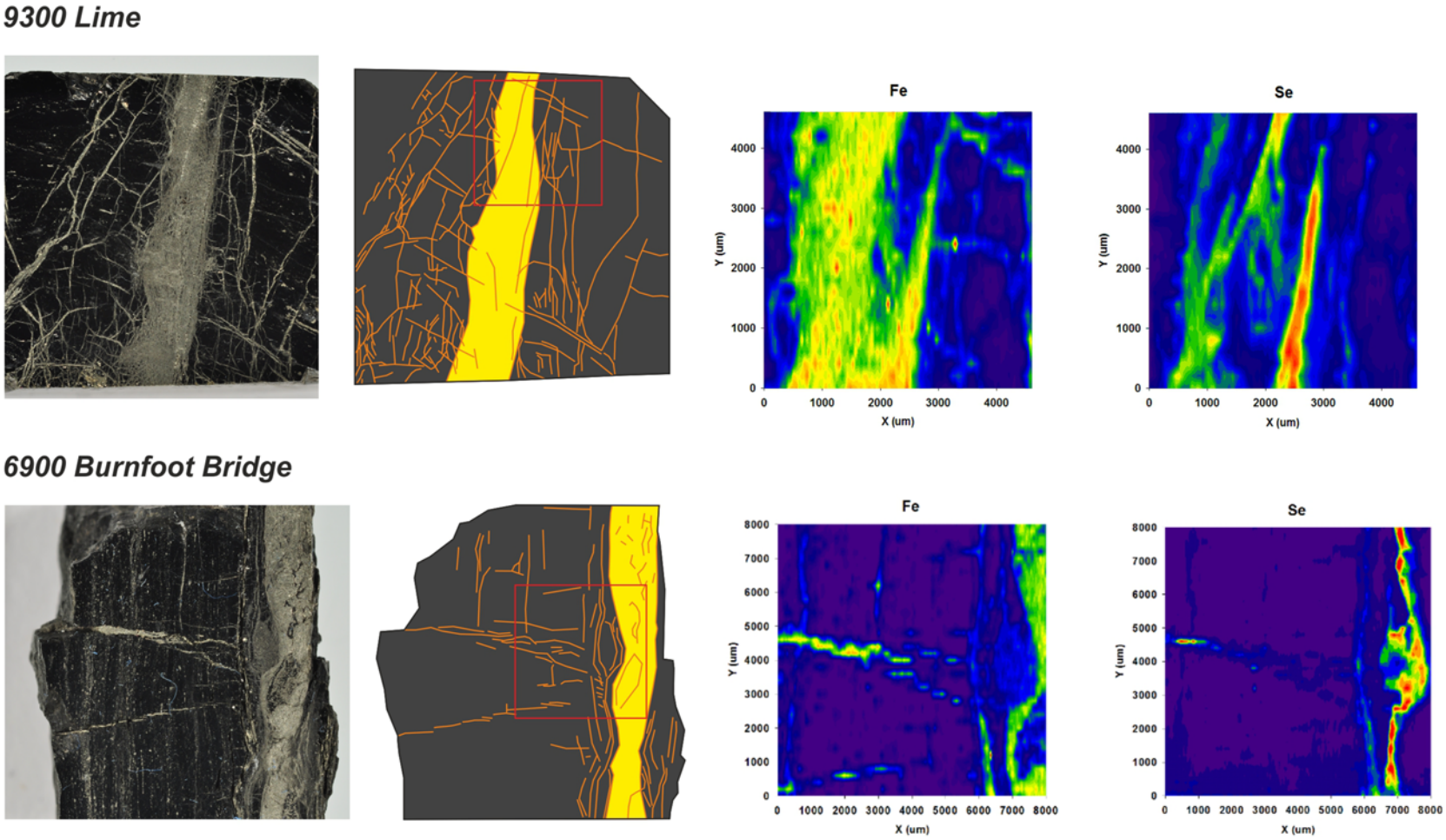

Fig. 4. Fe and Se laser ablation mapping of banded and cleat-filling pyrite in two Greenburn coal samples (map area depicted in schematic by red box). High Fe content defines all pyrite phases, while high Se concentrates in cleat-filling pyrite.

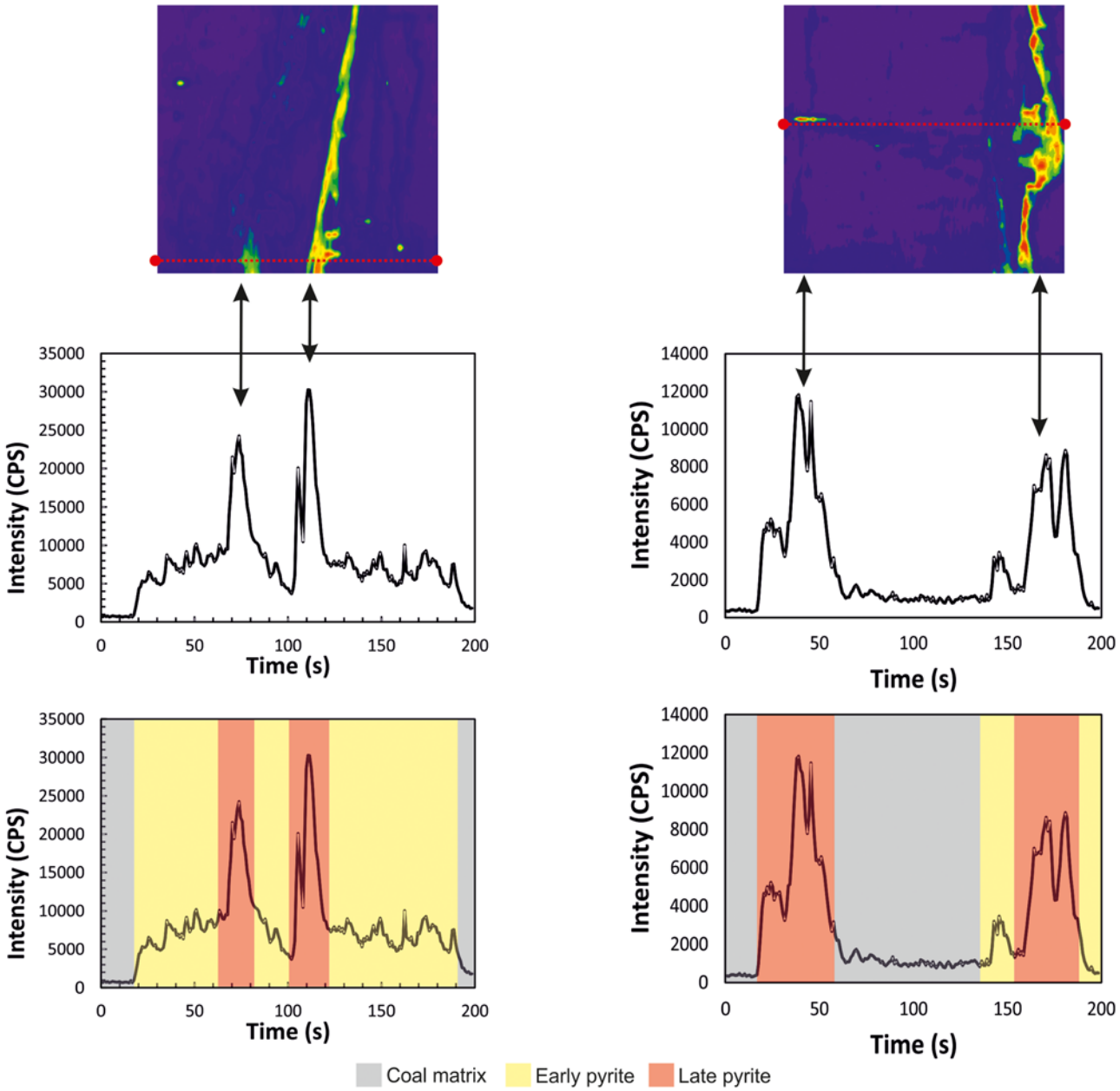

Fig. 5. Se LA-ICP-MS maps and corresponding line scan transects showing Se peak intensity. Large Se peaks correspond to cleat-filling pyrite perpendicular and parallel to banded pyrite.

Greenburn coals (David Richardson, pers. comm. 2017). Old Red Sandstone sedimentary rocks contain reduction spheroids that include selenide phases (Spinks *et al.* 2014). Selenide mineralization may have resulted from meteoric waters descending through fault planes into underlying sandstones in which microbially-induced reducing conditions prevailed. Reddening of coal beds in Ayrshire and NE Arran has been recognized previously (Bailey 1926; Mykura 1960; Wang 1992; Spinks *et al.* 2014), and attributed to mobilization of a fluid which also contains Se, with subsequent migration and mineralization in a reducing environment (Spinks *et al.* 2014). Total S content in Westphalian Coal Measures is largely reflected in pyrite content as opposed to the organic S content (e.g. Westphalian A and B Coal Measures of the Northumberland Coalfield; Turner & Richardson 2004). Variations in Se content may be linked to changes in the depositional environment, e.g. variable marine influence, with more marine-influenced coalfields showing higher S content (Turner & Richardson 2004), and therefore higher Se content.

Pyrite genesis

Variations in pyrite morphology (e.g. euhedral, massive banded and cleat-hosted pyrite) and S isotope compositions have previously been shown to reflect several generations of pyrite in coal formations (Dai *et al.* 2002; Turner & Richardson 2004). Cleats can also form at multiple stages as early- and late-cutting fracture sets and partings (Laubach *et al.* 1998; Rippon *et al.* 2006). Samples from the Greenburn mine show multiple generations of pyrite formation-banded syngenetic pyrite and epigenetic cleat-filling pyrite. Sulphur in coal may be derived from source plant material or from the bacterial reduction of aqueous sulphate.

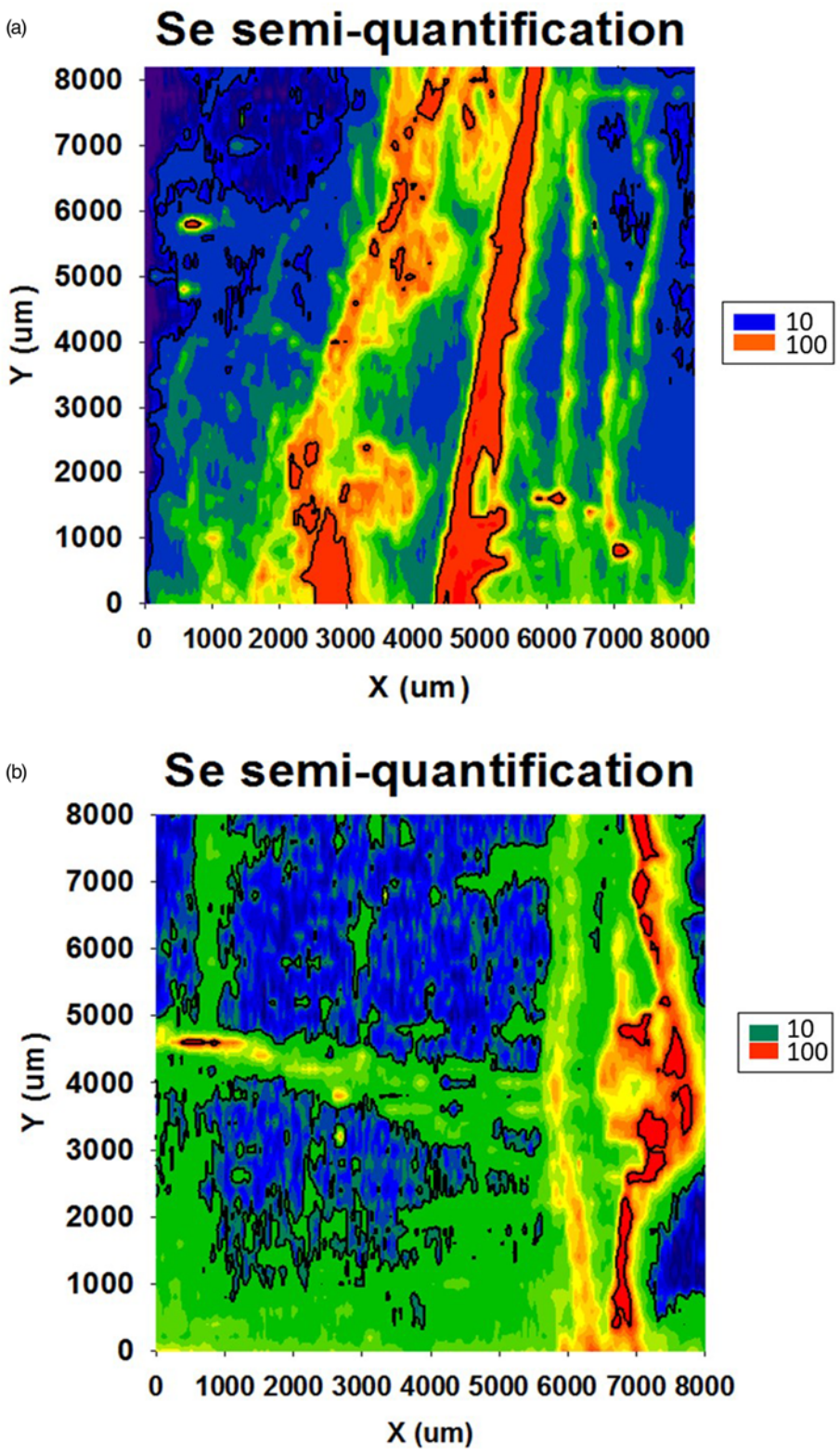

Fig. 6. Semi-quantification of Se content of pyrite and coal in (**a**) 9300 Lime and (**b**) 6900 K. Main Rider coals by LA-ICP-MS.

Sulphur isotope compositions can help to decipher whether pyrite generation (and resultant Se accumulation) is microbially-mediated (relating to syngenetic pyrite formation), and/or other mechanisms related to diagenesis and catagenesis (syngenetic to epigenetic pyrite; Claypool *et al.* 1980; Dai *et al.* 2002; McKay & Longstaffe 2003; Parnell *et al.* 2013). There is a high variation in $\delta^{34}S$ composition in Greenburn samples, with similar variability in the Northumberland Coalfield (−5.4 to +32.8‰ with an average of +5.1‰; Turner & Richardson 2004). One measured sample (from 6900 K. Main Rider) is in excess of +18‰, consistent with post-depositional addition of S (McKay & Longstaffe 2003; Turner & Richardson 2004). The range in S isotopic compositions indicates that pyrite may have formed by both microbial sulphate reduction (indicated by isotopically light compositions), and diagenetic fluids (heavier compositions), and therefore Se was also concentrated at multiple stages of pyrite generation.

Syngenetic pyrite may have formed from microbial sulphate reduction, as suggested by negative $\delta^{34}S$

Table 3. *Average (and maximum) sulphophile trace element content (ppm, Fe – %) of background coal, banded pyrite and cleat-filling pyrite for two Greenburn coal seams, analysed by LA-ICP-MS*

Sample	Ag	As	Bi	Cu	Fe	Hg	Pb	Se	Te
9300 Lime									
Background coal ($n = 4656$)	6.0	170.3	0.1	41.6	6.4	2.2	123.0	15.0	1.3
	(157.7)	(1428.0)	(7.5)	(692.0)	(41.9)	(14.4)	(2421.3)	(85.4)	(9.4)
Banded pyrite ($n = 3277$)	7.8	697.2	0.1	102.5	16.7	4.9	500.1	59.8	1.3
	(67.7)	(2002.2)	(10.6)	(394.7)	(76.6)	(15.0)	(1959.3)	(180.7)	(11.6)
Cleat pyrite ($n = 385$)	10.2	1750.5	0.1	191.7	28.9	10.0	979.2	157.0	0.8
	(39.3)	(3258.7)	(0.9)	(385.2)	(51.4)	(18.1)	(2432.7)	(266.0)	(2.9)
6900 Burnfoot Bridge									
Background coal ($n = 4068$)	2.8	56.0	0.1	18.3	3.7	1.4	94.3	8.6	1.7
	(96.0)	(590.0)	(3.0)	(290.8)	(40.2)	(14.6)	(1570.0)	(44.8)	(38.1)
Banded pyrite ($n = 1748$)	4.6	288.1	0.1	47.8	13.7	2.5	243.5	24.8	2.2
	(44.7)	(1532.3)	(3.1)	(313.1)	(57.8)	(13.9)	(2704.1)	(70.7)	(71.3)
Cleat pyrite ($n = 604$)	6.7	460.2	0.2	76.7	22.5	3.5	638.5	83.9	1.9
	(31.6)	(1397.4)	(18.4)	(209.3)	(43.2)	(26.3)	(2578.7)	(190.0)	(58.9)

Averages calculated from raw data points from each sample. *n*, Number of analyses.

compositions, but also from precipitation of Fe. Syngenetic pyrite formation may be multi-stage, due to variations in the availability and mobility of Fe in pore solutions during early diagenesis (Spears & Amin 1981; Spears & Caswell 1986). If reduced sulphur speciation activity and Fe mobility are low in pore solutions, sulphides may precipitate upon encountering reduced sulphur species, with some Fe^{2+} remaining in the system, depending upon HCO^{3-} availability (Spears & Amin 1981; Spears & Caswell 1986). Therefore, coupled with microbial sulphate reduction, Fe precipitation may form bedding-parallel bands and concretions over a period of time, resulting in multiple phases of syngenetic pyrite formation. Table 4 and Figure 7 show no clear pattern between $\delta^{34}S$ values and syngenetic or epigenetic pyrite. It may be anticipated that syngenetic pyrite would show lighter compositions and negative $\delta^{34}S$ values, indicating a bacterial origin, whereas epigenetic pyrite would show heavier compositions and positive $\delta^{34}S$ values. However, this is not observed, and the majority of samples for both syngenetic and epigenetic pyrite show positive $\delta^{34}S$ values. This suggests that most of the pyrite is unlikely to have been bacterial, and later pyrite is the result of hydrothermal mobilization and redeposition of earlier-formed pyrite, or that the syngenetic pyrite $\delta^{34}S$ signature was overprinted by later hydrothermal fluids. Vertical variation and an overall decrease in $\delta^{34}S$-values from Lower to Middle (and, to a lesser extent, Upper) Coal Measures may relate to proximity to overlying rocks or changing environmental conditions during deposition. The opposite trend has been noticed in low-sulphur Danville coals of Indiana, with $\delta^{34}S$-values progressively increasing upwards (Jiang *et al.* 2008). This progression was attributed to a closed system with limited sulphate supply and limited influence by seawater (Hoefs 2004; Jiang *et al.* 2008). The trend of decreasing $\delta^{34}S$-values in Greenburn coals may suggest an increasing seawater influence and sulphate supply.

Cleat formation and Se enrichment

LA-ICP-MS mapping reveals that although Se (and other trace elements; see Supplementary material) is concentrated in syngenetic pyrite, there is a distinction in trace element content between syngenetic and epigenetic pyrite. Although Se (along with other redox-sensitive trace elements) is commonly associated with syngenetic pyrite (absorbed from seawater and local pore waters), mapping reveals that there is a greater concentration in epigenetic cleat-filling pyrite (up to 266 ppm compared to 181 ppm in syngenetic pyrite, an average of 35% higher). This suggests that additional Se was mobilized during the later stages of pyrite formation, and that catagenetic fluids were responsible for high concentrations of Se and other trace elements in some coals. During the Late Visean, Namurian and Westphalian stages, syn-sedimentary tectonic movements and regional-scale dextral strike, oblique-slip movements were common (Browne & Monro 1989; Ritchie *et al.* 2003; Underhill *et al.* 2008; Leslie *et al.* 2016), with deformation in Ayrshire associated with ENE-trending faults (Leslie *et al.* 2016). Coal Measures were also affected by extensive post-

Table 4. *S isotope composition ($\delta^{34}S$) of pyrite from sampled Greenburn coal seams (stage of pyrite genesis also shown)*

Sampled seam	Pyrite genesis	$\delta^{34}S$ (‰)
6900 K. Main Rider	Syngenetic	9.0
	Epigenetic	9.9
	Syngenetic	8.9
	Syngenetic	18.4
	Syngenetic	7.1
	Syngenetic	7.6
	Syngenetic	7.4
8650 Eight Foot Upper	Syngenetic	3.8
	Epigenetic	6.1
8700 Five Foot Lower	Syngenetic	5.5
	Epigenetic	5.2
9300 Lime	Syngenetic	1.0
	Syngenetic	−4.0
	Epigenetic	−9.3
	Epigenetic	−11.1
9400 Little Cannel	Epigenetic	4.8
	Epigenetic	11.6
9450 Little Cannel Upper	Syngenetic	2.5
	Epigenetic	0.0
9600 Burnfoot Bridge	Epigenetic	−1.3
1940 Little Cannel Stringer	Syngenetic	−26.3

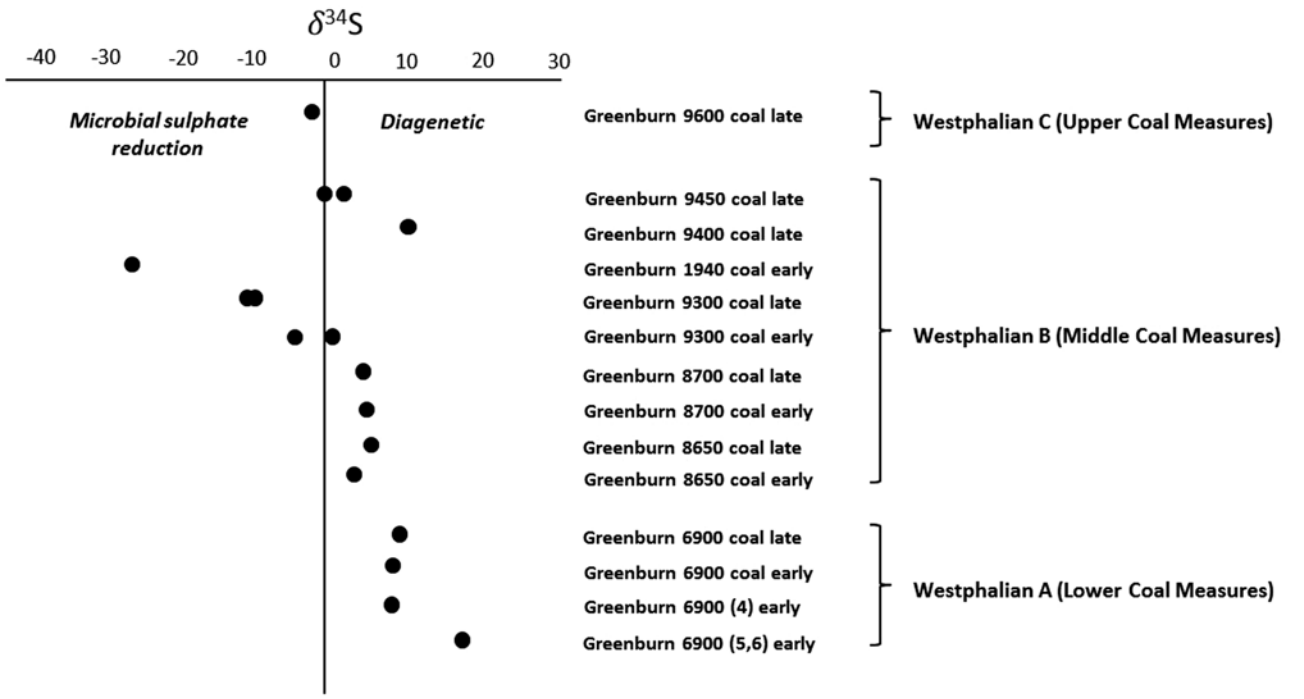

Fig. 7. S isotopic compositions of pyrite from sampled Greenburn coals, showing that pyrite predominantly formed by diagenetic processes, but some may also have formed due to microbial sulphate reduction, particularly in Westphalian B (Middle Coal Measures) coal seams.

Carboniferous, pre-Hercynian, deformation, resulting in further folding and fault development (Picken 1988). This resulted in a set of superimposed tectonic fractures in the coals, including the cleat fracture system. Cleats provide channels for fluid flow, and the host coal offers a source of S resulting from bacterial sulphate reduction (Hatch *et al.* 1976). The development of cleats therefore provides a locus for epigenetic pyrite precipitation and associated higher Se concentrations.

The concentrations of Se in epigenetic cleat-filling pyrite demonstrate that this element was freely available (at least on a regional scale) from mobile fluids during much of the Carboniferous Period. A high Pb content, associated with epigenetic cleat-filling pyrite precipitation, also relates to later deformation and fluid mobility, consistent with Pb-rich pyrite and Pb vein mineralization in Carboniferous rocks of SW Scotland (Pattrick 1985; Pattrick & Russell 1989). A number of factors are pivotal in the development of cleats and subsequent trace element concentrations in epigenetic pyrite. In the Midland Valley of Scotland, cleats result from both local structural developments during basin evolution, and differing phases of igneous activity (Rippon *et al.* 2006). The complex fault architecture of the Ayrshire region (particularly in close vicinity to Braehead and the Greenburn mine) are likely responsible for the local discordant brittle fracturing and high strain imposed on the Carboniferous rocks. Alteration and de-volatilization of the coals, as well as continued thermal maturation during burial, may also have helped to develop fractures in the coals and impact on preferential accumulation of elements, such as Se, in pyrite. A potential source and fluid distribution mechanism for enriched levels of Se, compared to UK and worldwide concentrations in coals, may have been in the Permian dolerite sills that intruded the sequence.

Comparison of associated trace elements to other coal-bearing sequences

Previous studies have highlighted higher trace element concentrations resulting from late stage catagenetic/epigenetic fluids in coals (Gayer *et al.* 1999; Goldhaber *et al.* 2000; Dai *et al.* 2005, 2006; Yudovich & Ketris 2005*a*; Hower *et al.* 2007; Spears & Tewalt 2009). The enrichment of trace elements in the later cleat-filling pyrites of Ayrshire demonstrated in this study agrees with these observations.

In previous studies of UK coals, trace element concentrations have been shown to increase in the later stages of cleat infill (Spears & Amin 1981; Spears & Caswell 1986; White *et al.* 1989; Spears & Tewalt 2009). This has been attributed to possible time-dependent increases in concentrations, and a larger grain size in cleats providing a greater opportunity for element segregation compared to the early diagenetic pyrite. For instance, Spears & Caswell (1986) showed that Co, Cu, Ni, Pb and Zn are higher in later pyrite cleats than in earlier pyritic nodules (Lea Hall and Littleton collieries, Staffordshire). Here, earlier-formed pyrite contained 35–150 ppm Cu and 25–30 ppm Pb, and later cleat-filling pyrite contained 685–1815 ppm Cu and 425–665 ppm Pb (Spears & Caswell 1986). By comparison, pyrite from the coals in this study contains higher concentrations of Cu and Pb. Syngenetic pyrite in Ayrshire coals contains *c.* 48–102 ppm Cu and *c.* 243–500 ppm Pb, whereas epigenetic cleat-filling pyrite contains *c.* 76–191 ppm Cu and *c.* 425–665 ppm Pb.

Pyrite is the main carrier of As in coals (Bayet & Slosse 1919; Spears & Zheng 1999) and has previously been shown to be enriched in later-formed pyrite (e.g. Bayet & Slosse 1919; Finkelman 1980; Spears & Zheng 1999; Goldhaber *et al.* 2000; Ding *et al.* 2001; Diehl *et al.* 2004; Yudovich & Ketris 2005*a*) as a result of catagenetic hydrothermal fluids

or As-bearing groundwaters (Goldhaber *et al.* 2000; Yudovich & Ketris 2005*a*). For instance, Yudovich & Ketris (2005*a*) described coarse, later-formed massive pyrite bands of eastern Kentucky coals containing higher As than earlier-formed euhedral and framboidal pyrite generations. Trace element concentrations in pyrite of Pennsylvanian coals in the Appalachian Basin showed depletion of As and Hg and enrichment of Pb and Ni in earlier-formed compared to later-formed pyrite (Diehl *et al.* 2004). Pyrite in late-stage veins was shown to contain As-rich growth zones, attributed to a probable epigenetic hydrothermal origin (Diehl *et al.* 2004). In samples of West Virginia massive pyrite, As averaged 1700 ppm ($n = 24$), while Alabama pyrite veins contained the highest concentrations of Hg (Diehl *et al.* 2004). Although Hg has a strong affinity for humic matter and may accumulate in peats and lignites, and therefore early-formed diagenetic pyrite, Hg enrichment in coals is typically a catagenetic hydrothermal process, e.g. the Nikitovka (Ukraine), Warrior (USA) and Guizhou (China) basins (Yudovich & Ketris 2005*b*). By comparison, pyrite in Ayrshire coals shows enriched concentrations of As in epigenetic cleat-filling pyrite (average concentrations of *c.* 460–1750 ppm, similar to concentrations in West Virginia coal massive pyrite; Diehl *et al.* 2004), where concentrations of Hg are also higher.

Economic and environmental implications

Whole-rock concentrations of Se, up to 15.8 ppm, and pyrite content of up to 200 ppm are not high enough to be considered economically viable for extraction. However, the concentrations of Se and other trace elements in cleat-filling pyrite, and the relationship of these to brittle deformation and intrusive activity, mean that other areas of the world, such as the coalfields of Australia, USA, Russia and China, may also host high Se content. Seleniferous coals have been shown to cause environmental issues in countries such as China (Cheng 1980; Mao *et al.* 1988; Su *et al.* 1990; Zheng *et al.* 1992, 1999; Finkelman *et al.* 2002; He *et al.* 2002; Lei 2012; Zhu *et al.* 2012) and elsewhere. The Se values for Chinese coals are, on average, 4.2 ppm, with a maximum of 30 ppm (Bragg *et al.* 1998). The environmental ramifications of high Se in Chinese coals draw attention to areas that show similar or higher concentrations in coals worldwide, including the Greenburn coals. The main environmental issue associated with Se that might threaten the Ayrshire region is elevated levels in groundwater and streams (e.g. coal mine drainage and ochre development) in the vicinity of both current and former coal workings. However, a study of Se concentrations in Scottish soils conducted from 2007 to 2009 by Shand *et al.* (2012) suggests that this threat is negligible. Shand *et al.* (2012) sampled 688 soils and, although the distribution of Se showed a propensity for higher concentrations in the west of Scotland, these were more commonly associated with mixed metamorphic and igneous rocks. The Greenburn mine is centred on a soil association derived from Carboniferous sandstones, shales, coals and limestones, with Se soil content below the limit of detection (<0.06 ppm). In the larger exposed Ayrshire coalfield Se content in soils reaches a maximum of 2.93 ppm (Shand *et al.* 2012).

Conclusions

Our results indicate that the high Se content of Greenburn coals relates to the evolution of a multi-stage pyrite mineralization, including deposition, diagenesis and catagenesis of the host rocks, intrusive igneous activity, deformation and fluid mobilization. Selenium may have been sourced from sulphidic Dalradian rocks that have been reported to contain high trace element concentrations. Greenburn surface mine coals are characterized by syngenetic concretionary pyrite and later-formed, epigenetic cleat-filling pyrite. Sulphur isotope compositions indicate that pyrite may have formed by microbial sulphate reduction, diagenetic processes and/or hydrothermal fluids. Initial Se sequestration is associated with syngenetic mineralization, with additional Se from fluids mobilized during later epigenetic pyrite formation. Cleats in local fractures provided channels for later fluid flow and precipitation of comparatively high-Se pyrite. Understanding the processes responsible for the development of Se-rich pyritic coals in Ayrshire may help to identify similar processes concentrating strategic elements in coal worldwide, important both for identifying potentially exploitable resources and predicting the environmental impact of weathering and processing in coal.

Acknowledgements The authors wish to thank Kier Group for site access and providing seam-constrained Greenburn Surface Mine Complex coal samples. We thank David Richardson (Kier Group) for sharing his knowledge of the Greenburn site and local geology, as well as additional average sulphur content seam data. Critical comments from David A. Spears, Yakov E. Yudovich and Colin J.R. Braithwaite are gratefully acknowledged.

Funding Funding provided by NERC Security of Supply programme (grant NE/L001764/1).

Scientific editing by Colin Braithwaite

Correction Notice: This article was made Open Access.

References

Ayres, R.U. & Talens Peiró, L. 2013. Material efficiency: rare and critical metals. *Philosophical Transactions of the Royal Society*, **A371**, 1–21.

Bailey, E.B. 1926. Subterranean penetration by a desert climate. *Geological Magazine*, **63**, 276–280.

Bayet, A. & Slosse, A. 1919. Arsenical intoxication in the coal and coal-derivative industries. *Comptes rendus de l'Académie des Sciences*, **168**, 704–706.

Bottrell, S.H., Louie, P.K.K., Timpe, R.C. & Hawthorne, S.B. 1994. The use of stable sulfur isotope ratio analysis to assess selectivity of chemical analyses and extractions of forms of sulfur in coal. *Fuel*, **73**, 1578–1582.

Bragg, L.J., Oman, J.K., Tewalt, S.J., Oman, C.L., Rega, N.H., Washington, P.M. & Finkelman, R.B. 1998. *U.S. Geological Survey Coal Quality (COALQUAL) Database: Version 2.0*. US Geological Survey Open File Report, 97-134, CD-ROM.

British Geological Survey (BGS) online 2017. Scotland's Carboniferous legacy landscapes, http://www.bgs.ac.uk/research/ukgeology/scotland/carboniferousLegacyLandscapes.html [last accessed 26 July 2017].

Browne, M.A.E. & Monro, S.K. 1989. Evolution of the coal basins of Central Scotland. *In: Compte Rendu XIme Congrès International de Stratigraphie et de Géologie du Carbonifère*, 1987, Beijing. Nanjing University Press, **5**, 1–19.

Cheng, J. 1980. The preliminary investigation report of selenium intoxication in Ziyang County of Shanxi Province (in Chinese with English abstract). *Journal of Shanxi Agricultural Sciences*, **6**, 17.

Claypool, G.E., Holser, W.T., Kaplan, I.R., Sakai, H. & Zak, I. 1980. The age curves of sulfur and oxygen isotopes in marine sulfate and their mutual interpretation. *Chemical Geology*, **28**, 199–260.

Dai, S., Ren, D., Tang, Y., Shao, L. & Li, S. 2002. Distribution, isotopic variation and origin of sulphur in coals in the Wuda coalfield, Inner Mongolia, China. *International Journal of Coal Geology*, **51**, 237–250.

Dai, S., Chou, C.-L., Yue, M., Luo, K. & Ren, D. 2005. Mineralogy and geochemistry of a late Permian coal in the Dafang Coalfield, Guizhou, China: influence from siliceous and iron-rich calcic hydrothermal fluids. *International Journal of Coal Geology*, **61**, 241–258.

Dai, S., Sun, Y. & Zeng, R. 2006. Enrichment of arsenic, antimony, mercury, and thallium in a Late Permian anthracite from Xingren, Guizhou, Southwest China. *International Journal of Coal Geology*, **66**, 217–226.

Diehl, S.F., Goldhaber, M.B. & Hatch, J.R. 2004. Modes of occurrence of mercury and other trace elements in coals from the warrior field, Black Warrior Basin, Northwestern Alabama. *International Journal of Coal Geology*, **59**, 193–208.

Ding, Z., Zheng, B. *et al.* 2001. Geological and geochemical characteristics of high arsenic coals from endemic arsenosis areas in southwestern Guizhou Province, China. *Applied Geochemistry*, **16**, 1353–1360.

Dron, R.W. 1925. Notes on cleat in the Scottish coalfield. *Transactions of the Institution of Mining and Metallurgy*, **70**, 115–117.

Fielding, C.R. 1982. *Sedimentology and stratigraphy of the Durham Coal Measures and comparison with other British Coalfields*. PhD thesis, University of Durham.

Finkelman, R.B. 1980. *Modes of occurrence of trace elements in coal*. PhD thesis, University of Maryland.

Finkelman, R.B., Harvey, B. & Zheng, B.S. 1999. Health impacts of domestic coal use in China. *Proceedings of the National Academy of Sciences of the United States of America*, **76**, 3427–3431 (March, Colloquium paper).

Finkelman, R.B., Orem, W. *et al.* 2002. Health impacts of coal and coal use: possible solutions. *International Journal of Coal Geology*, **50**, 425–443.

Gayer, R.A., Rose, M., Dehmer, J. & Shao, L.-Y. 1999. Impact of sulphur and trace element geochemistry on the utilization of marine-influenced coal-case study from South Wales Variscan foreland basin. *International Journal of Coal Geology*, **40**, 151–174.

Goldhaber, M.B., Irwin, E.R., Atkins, J.B., Lee, R., Zappia, H., Black, D.D. & Finkelman, R.B. 2000. Environmental impact of elevated arsenic in Southern Appalachian Basin coals. *Metal Ions in Biology and Medicine*, **6**, 38–40.

Hatch, J.R., Gluskoter, H.J. & Lindahl, P.C. 1976. Sphalerite in coals from the Illinois Basin. *Economic Geology*, **71**, 613–624.

He, B., Liang, L. & Jiang, G. 2002. Distributions of arsenic and selenium in selected Chinese coal mines. *The Science of the Total Environment*, **296**, 19–26.

Hendry, M.J., Biswas, A., Essilfie-Dughan, J., Chen, N., Day, S.J. & Barbour, S. L. 2015. Reservoirs of Selenium in coal waste rock: Elk Valley, British Columbia, Canada. *Environmental Science and Technology*, **49**, 8828–8236.

Hoefs, J. 2004. *Stable Isotope Geochemistry,* 5th revised and updated edn. Springer-Verlag, Berlin, 63–69.

Hower, J.C., Ruppert, L.F. & Eble, C.F. 2007. Lateral variation in geochemistry, petrology, and palynology in the Elswick coal bed, Pike County, Kentucky. *International Journal of Coal Geology*, **69**, 165–178.

Jiang, Y., Elswick, E.R. & Mastalerz, M. 2008. Progression in sulfur isotopic compositions from coal to fly ash: Examples from single-source combustion in Indiana. *International Journal of Coal Geology*, **73**, 273–284.

Ketris, M.P. & Yudovich, Y.E. 2009. Estimations of Clarkes for carbonaceous biolithes: world averages for trace element contents in black shales and coals. *International Journal of Coal Geology*, **78**, 135–148.

Kier Mining 2009. *Greenburn South – Generalised Strata Section*, scale 1:1600. A3 Drawing No 6215A/S/ES/0302.

Large, R.R., Halpin, J.A. *et al.* 2014. Trace element content of sedimentary pyrite as a new proxy for deep-time ocean-atmosphere evolution. *Earth and Planetary Science Letters*, **389**, 209–220.

Laubach, S.E., Marrett, R.A., Olson, J.E. & Scott, A.R. 1998. Characteristics and origins of coal cleat: A review. *International Journal of Coal Geology*, **35**, 175–207.

Lebon, J.H.G. 1933. The development of the Ayrshire coalfield. *Scottish Geographical Magazine*, **49**, 138–154.

Lei, W. 2012. *Selenium in Chinese coal: Distribution, mode and occurrence and environmental geochemistry*. PhD thesis, City University of Hong Kong.

Lemly, A.D. 2004. Aquatic selenium pollution is a global environmental safety issue. *Ecotoxicology and Environmental Safety*, **59**, 44–56.

Leslie, A.G., Browne, M.A.E., Cain, T. & Ellen, R. 2016. From threat to future asset – The legacy of opencast surface-mined coal in Scotland. *International Journal of Coal Geology*, **164**, 123–133.

Lusty, P.A.J. & Gunn, A.G. 2014. Challenges to global mineral resource security and options for future supply. *In:*Jenkin, G.R.T., Lusty, P.A.J., McDonald, I., Smith, M. P., Boyce, A.J. & Wilkinson, J.J. (eds) *Ore Deposits in an Evolving Earth*. Geological Society of London, Special Publications, **393**, 265–276, https://doi.org/10.1144/SP393.13

Mao, D., Su, H., Wang, Y. & Luo, G. 1988. Preliminary study of selenium intoxication caused by weathering and burning of high selenium carbonaceous shale. *Journal of Chinese Endemic Diseases*, **7**, 297–299.

McDonald, L.E. & Strosher, M.M. 1998. *Selenium mobilization from surface coal mining in the Elk River Basin, British Columbia: A survey of water, sediment and biota*. Pollution Prevention Ministry of Environment, Lands and Parks Report, Kootenay Region, Canbrook, British Columbia.

McKay, J.L. & Longstaffe, F.J. 2003. Sulphur isotope geochemistry of pyrite from the upper Cretaceous Marshybank Formation, Western Interior Basin. *Sedimentary Geology*, **157**, 175–195.

Mykura, W. 1960. The replacement of coal by limestone and the reddening of Coal Measures in the Ayrshire Coalfield. *Bulletin of the Geological Survey of Great Britain*, **16**, 131–155.

Parnell, J., Boyce, A.J., Hurst, A., Davidheiser-Kroll, B. & Ponicka, J. 2013. Long term geological record of a global deep subsurface microbial habitat in sand injection complexes. *Scientific Reports*, **3**, **1828**, https://doi.org/10.1038/srep01828

Pattrick, R.A.D. 1985. Pb–Zn and minor U mineralization at Tyndrum, Perthshire. *Mineralogical Magazine*, **49**, 671–681.

Pattrick, R.A.D. & Russell, M.J. 1989. Sulphur isotopic investigation of Lower Carboniferous vein deposits of the British Isles. *Mineralium Deposita*, **24**, 148–153.

Picken, G.S. 1988. The concealed coalfield at Canonbie: an interpretation based on boreholes and seismic surveys. *Scottish Journal of Geology*, **24**, 61–71, https://doi.org/10.1144/sjg24010061

Richey, J.E., Wilson, G.V., Anderson, E.M. & Dinham, C.H. 1925. Economic geology of the Ayrshire Coalfields. Area 1: Kilbirnie, Dalry, and Kilmaurs. *Memoirs of the Geological Survey, Scotland*, **91**.

Rippon, J.H., Ellison, R.A. & Gayer, R.A. 2006. A review of joints (cleats) in British Carboniferous coals: indicators of palaeostress orientation. *Proceedings of the Yorkshire Geological Society*, **56**, 15–30, https://doi.org/10.1144/pygs.56.1.15

Ritchie, J.D., Johnson, H., Browne, M.A.E. & Monaghan, A.A. 2003. Late Devonian-Carboniferous tectonic evolution within the Firth of Forth, Midland Valley; as revealed from 2D seismic reflection data. *Scottish Journal of Geology*, **39**, 121–134, https://doi.org/10.1144/sjg39020121

Seal, R.R., II. 2006. *Sulfur Isotope Geochemistry of Sulfide Minerals*. USGS Staff – Published Research. Paper 345.

Shand, C.A., Eriksson, J., Dahlin, A.S. & Lumsdon, D.G. 2012. Selenium concentrations in national inventory soils from Scotland and Sweden and their relationship with geochemical factors. *Journal of Geochemical Exploration*, **121**, 4–14.

Smith, R.A., Bide, T., Hyslop, E.K., Smith, N.J.P., Coleman, T. & McMillan, A. A. 2008. *Mineral Resource map for North Ayrshire, East Ayrshire and South Ayrshire*. BGS map OR/08/014.

Spears, D.A. 2015. The geochemistry and mineralogy of high-S coals, with examples mainly from the Yorkshire-Nottinghamshire coalfields, UK: an overview. *Proceedings of the Yorkshire Geological Society*, **60**, 204–226, https://doi.org/10.1144/pygs2015-356

Spears, D.A. & Amin, M.A. 1981. Geochemistry and mineralogy of marine and non-marine Namurian black shales from the Tansley Borehole, Derbyshire. *Sedimentology*, **28**, 407–417.

Spears, D.A. & Caswell, S.A. 1986. Mineral matter in coals: Cleat minerals and their origin in some coals from the English Midlands. *International Journal of Coal Geology*, **6**, 107–125.

Spears, D.A. & Tewalt, S.J. 2009. The geochemistry of environmentally important trace elements in UK coals, with special reference to the Parkgate Coal in the Yorkshire – Nottinghamshire Coalfield, UK. *International Journal of Coal Geology*, **80**, 157–166.

Spears, D.A. & Zheng, Y. 1999. Geochemistry and origin of elements in some UK coals. *International Journal of Coal Geology*, **38**, 161–179.

Spinks, S.C., Parnell, J. & Still, J.W. 2014. Redox-controlled selenide mineralization in the Upper Old Red Sandstone. *Scottish Journal of Geology*, **50**, 173–182, https://doi.org/10.1144/sjg2013-014

STDA Selenium-Tellurium Development Association 2013. Sources of selenium and tellurium, http://www.stda.org/se_te.html

Su, H., Yan, L., Rao, S., Jian, X. & Mao, D. 1990. Investigation of the cause of the origination of the environmental selenium and high selenium area in the Exi Autonomous Prefecture of Hubei Province. *Environmental Science*, **11**, 86–89.

Swaine, D.J. 1990. *Trace Elements in Coal*. Butterworths, London, 178–386.

Talens Peiró, L., Méndez, G.V. & Ayres, R.U. 2011. Rare and critical metals as by-products and the implications for future supply. *INSTEAD Facility and Research Working Paper*. 2011/129/EPS/TOM/ISIC.

Thirlwall, M.F. 1986. Lead isotope evidence for the nature of the mantle beneath Caledonian Scotland. *Earth and Planetary Science Letters*, **80**, 55–70.

Turner, B.R. & Richardson, D. 2004. Geological controls on the sulphur content of coal seams in the Northumberland Coalfield, Northeast England. *International Journal of Coal Geology*, **60**, 169–196.

Tyrrell, G.W. 1928. On some dolerite-sills containing analcite-syenite in Central Ayrshire. *Quarterly Journal of the Geological Society of London*, **84**, 540–569, https://doi.org/10.1144/GSL.JGS.1928.084.01-04.20

UKERC UK Energy Research Centre 2012. *Energy Materials Availability Handbook*. UK Energy Research Centre, London, UK.

Underhill, J.R., Monaghan, A.A. & Browne, M.A.E. 2008. Controls on structural styles, basin development and petroleum prospectivity in the Midland Valley of Scotland. *Marine and Petroleum Geology*, **25**, 1000–1022.

Walker, F. & Patterson, E.M. 1959. A differentiated boss of alkali dolerite from Cnoc Rhaonastil, Islay. *Mineralogical Magazine*, **32**, 140–152.

Wang, W.H. 1992. Origin of reddening and secondary porosity in Carboniferous sandstones, Northern Ireland. *In:* Parnell, J. (ed.) *Basins on the Atlantic Seaboard: Petroleum Geology, Sedimentology and Basin Evolution*. Geological Society of London, Special Publications, **62**, 243–254, https://doi.org/10.1144/GSL.SP.1992.062.01.20

Waters, C.N., Browne, M.A.E., Dean, M.T. & Powell, J.H. 2007. Lithostratigraphical framework for Carboniferous successions of Great Britain (Onshore). *British Geological Survey Research Report,* RR/07/01.

White, R.N., Smith, J.V., Spears, D.A., Rivers, M.L. & Sutton, S.R. 1989. Analysis of iron sulphides from U.K. coal by synchrotron radiation X-ray fluorescence. *Journal of the Institute of Fuel*, **68**, 1480–1486.

Willan, R.C.R. 1980. Stratabound sulphide mineralisation in the Dalradian supergroup of the Grampian Highlands, Scotland. *Norges Geologiske Vndersokelse*, **360**, 241–258.

Willan, R.C.R. & Hall, A.J. 1979. Sphalerite geobarometry and trace-element studies on stratiform sulphide from McPhun's Cairn, Loch Fyne, Argyll, Scotland. *Transactions of the Institutions of Mining and Metallurgy*, **89**, B31–B40.

Woodhouse, M., Goodrich, A., Margolis, R., James, T.L., Lokanc, M. & Eggert, R. 2013. Supply-chain dynamics of Tellurium, Indium, and Gallium within the context of PV manufacturing costs. *IEEE Journal of Photovoltaics*, **3**, 833–837.

Yudovich, Y.E. & Ketris, M.P. 2005*a*. Arsenic in coal: a review. *International Journal of Coal Geology*, **61**, 141–196.

Yudovich, Y.E. & Ketris, M.P. 2005*b*. Mercury in coal: a review. Part. 1. Geochemistry. *International Journal of Coal Geology*, **62**, 107–134.

Yudovich, Y.E. & Ketris, M.P. 2006. Selenium in coal: a review. *International Journal of Coal Geology*, **67**, 112–126.

Yudovich, Y.E. & Ketris, M.P. 2015. *Geochemistry of Coal. Occurrences and Environmental Impacts of Trace Elements Coal Production and Processing Technology*. CRC Press, Boka Raton.

Zheng B.S., Hong Y. *et al.* 1992. The Se-rich carbonaceous siliceous rock and endemic selenosis in southwest Hubei, China. *Chinese Science Bulletin*, **37**, 1725–1729.

Zheng, B.S., Ding, Z. & Huang, R. 1999. Issues of health and disease relating to coal use in southwest China. *International Journal of Coal Geology*, **40**, 119–132.

Zhu, J.M., Johnson, T.M., Finkelman, R.B., Zheng, B.S., Sýkorová, I. & Pešek, J. 2012. The occurrence and origin of selenium minerals in Se-rich stone coals, spoils and their adjacent soils in Yutangba, China. *Chemical Geology*, **330–331**, 27–38.